Journal of Current Research and Studies

Volume 03 Issue 04 July-August 2026
https://journalcurrentresearch.com/
ISSN:3048-9911

OPEN ACCESS

*Correspondence
O. A. ADETOYE

Article Received
31/07/2026
Accepted
04/08/2026
Published
07/08/2026

Works Cited

O. A. ADETOYE, A. ABUBAKAR, I. M. LAWAL &O. O. OLUBAJO., (2026). Biogenic Calcite Production from Bacillus Subtilis: Characterization and Potential for Sustainable Self-healing Construction Materials. *Journal of Current Research and Studies*, 3(4), 100-106.

Biogenic Calcite Production from Bacillus Subtilis: Characterization and Potential for Sustainable Self-healing Construction Materials

O. A. ADETOYE[1], A. ABUBAKAR[2], I. M. LAWAL[3] &O. O. OLUBAJO[4]
[1]Civil Engineering Department, Abia State University Uturu, Abia State, Nigeria
[2,3]Civil Engineering Department, Abubakar Tafawa Balewa University Bauchi, Nigeria
[4]Chemical Engineering Department, Abubakar Tafawa Balewa University Bauchi, Nigeria

ABSTRACT

The self-healing mechanism in bio-concrete is attributed to Microbial Induced Calcium Carbonate Precipitation (MICCP). However, direct confirmation of the precipitated phase is required. This study identified crystals harvested from 90-day bio-concrete containing Bacillus subtilis and rice husk ash (RHA) using SEM, EDX and XRD.SEM revealed rhombohedral crystals with well-defined facets diagnostic of calcite, forming cluster-like networks that bridged pores and cracks. EDX showed Ca and C at 35.28% and 37.76% respectively, giving a Ca:C ratio of 1:1.07, within the ± 15% tolerance for CaCO3 confirmation. The spectrum displayed C Kα, O Kα and Ca Kα peaks consistent with CaCO3. XRD confirmed the phase as calcite with sharp peaks at $2\theta = 30.018^{o}$ (104), 36.52^{o}, 39.93^{o}, 43.72^{o}, 48.09^{o} and 49.14^{o}. Quantitative analysis showed 83(4)% calcite with minor albite and quartz. The (104) peak gave an average crystallite size of 28.6 nm by the Debye-Scherrer equation. Absence of aragonite and vaterite confirmed exclusive calcite formation. Thus, rhombohedral morphology, 1:1 Ca:C stoichiometry, Ca-C-O signature, and calcite XRD pattern confirm that B. subtilis precipitated calcite through MICCP, responsible for pore filling and crack bridging in RHA-modified bio-concrete.

KEYWORDS:

Bio-concrete, Bacillus subtilis, Rice Husk Ash, Calcite, MICCP, SEM, EDX, XRD

1.0 INTRODUCTION

Concrete is prone to micro-cracking due to its low tensile strength, which increases permeability and reduces long-term durability [1]. Bio-concrete addresses this limitation through Microbial Induced Calcium Carbonate Precipitation (MICCP), where ureolytic bacteria such as Bacillus subtilis precipitate CaCO3 to autonomously seal cracks [2][3]. The effectiveness of MICCP depends on the type, morphology, and chemical composition of the precipitated calcium carbonate. Calcium carbonate can exist in several polymorphs, including calcite, vaterite, and aragonite, with calcite being the most thermodynamically stable and mechanically favorable for crack bridging [4]. The incorporation of mineral admixtures such as rice husk ash (RHA) can influence crystal formation [5]. SEM imaging often shows crystal deposits in healed cracks; visual observation alone is insufficient to confirm MICCP. Chemical validation through elemental analysis is necessary to distinguish microbially precipitated calcite from residual cement hydration products [6]. Energy-Dispersive X-ray (EDX) spectroscopy provides a stoichiometric Ca:C ratio that serves as a fingerprint for CaCO3 [7]. The aim of this study is to provide conclusive evidence of MICCP in bio-concrete by analyzing the morphology and elemental composition of calcite harvested from healed pores of B. subtilis and RHA-modified concrete. This direct validation is critical to confirming that the observed self-healing is microbially driven rather than autogenous.

2.0 LITERATURE REVIEW

MICCP involves bacterial urease activity that hydrolyzes urea to produce carbonate ions, which react with calcium ions to precipitate CaCO3 within concrete pores and cracks. Bacillus subtilis is widely used due to its ability to form endospores and survive the high alkalinity of concrete [8]. The precipitated CaCO3 reduces porosity, increases density, and restores mechanical integrity [9] [10]. The morphology of precipitated CaCO3 is a key indicator of the precipitation mechanism. [4] reported that bacterial isolates frequently induce cubic, rhombic, and polygonal plate-like calcite morphologies, with rhombohedral crystals representing the stable calcite form. They also observed that spherical particles initially formed around bacterial cells transformed into well-defined rhombohedra within 7 days. Rhombohedral calcite provides mechanical interlocking that enhances crack closure and matrix strength, whereas spherical vaterite is metastable [4].

EDX analysis is a standard method for confirming CaCO3 precipitation in bio-concrete. SEM and EDX validated bacteria calcite, reporting high-intensity peaks for carbon, calcium, and oxygen [6] and also, elemental compositions of 34.5% Ca and 36.2% C, approximating a 1:1 ratio as proof of MICCP was reported by [5]. It was noted that EDX ratios within ± 15% of 1:1 is accepted as confirmation of CaCO3, despite underestimation of light elements [6]. In contrast, control concrete typically shows dominant Ca and Si peaks with weak carbon, reflecting C–S–H gel rather than carbonate [11]. RHA contributes reactive silica that undergoes pozzolanic reaction with calcium hydroxide to form additional C–S–H gel. It also provides micro-filler effects and nucleation sites that promote calcite precipitation. Trace elements such as Si, P, and K detected in MICP products are often attributed to RHA and bacteria growth media [4].

3.0 MATERIALS AND METHOD

Grade 42.5 Portland Limestone Cement, fine and coarse aggregates, potable water, and Conplast SP430 superplasticizer were used to prepare M25 grade concrete [12]. Rice husk ash was produced by incinerating rice husk at 750°C and sieving through 150 µm. Bacillus subtilis was cultured in nutrient broth and Luria-Bertani medium at 37°C for 24 – 48 h and concentrated to 6×10^6 CFU/mL. Bio-concrete specimens were cast with 6% RHA as cement replacement and 6 McFarland B. subtilis suspension. Specimens were water-cured for 90 days. After 90 days of curing, bio-concrete specimens with induced micro-cracks were split open. Whitish crystalline deposits observed within healed pores were physically harvested for analysis. The harvested crystals were mounted on aluminum stubs, sputter-coated with gold, and examined using a Phenom SEM at 15 kV and 500× magnification per ASTM C1723 [13] – [16]. Elemental composition was determined using EDX with a 10 s acquisition time. The Ca:C atomic ratio was calculated to assess stoichiometry.

4.0 RESULTS AND DISCUSSION

4.1 Precipitated Calcite

Visual monitoring of the crack zones for over 56 days, presented in Plate I: Induced Cracks in Concrete and Plate II: Calcite Formation in Cracks, provides direct evidence of the healing process.

Crack healing and Calcite formation

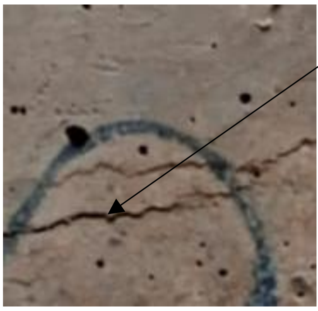

Plate I: Induced Crack in Concrete

Plate II: Calcites in Cracks

4.2 SEM Analysis of Precipitated Calcite

To conclusively identify the crystals observed in Plate II and prove that the self-healing mechanism was MICP-driven, pure calcite was physically harvested from healed pores of 90-day bio-concrete. The harvested crystals were analyzed using SEM for morphology and the result is presented in Plate III

Faceted Rhombohedral Crystals

Plate III: SEM Image of Pore Structure of Precipitated Calcite

Plate III shows distinct rhombohedral and cubic crystals with well-defined facets and smooth surfaces precipitated within pore spaces. The matrix is dominated by small, rounded, or sub-spherical grains. This morphology is a strong indicator of vaterite (a metastable polymorph of calcium carbonate). The individual calcium carbonate granules have aggregated into a continuous, porous network. This cohesive, cluster-like structure explains how bioconcrete effectively fills micro-cracks and binds sand particles together. The morphology matches the 3 classic calcite crystal habits reported in MICP studies. Nasser et al/ [4] identified "cubic, rhombic, and polygonal plate-like" as the most frequently induced calcite morphologies by bacteria isolates, with rhombohedral calcite being the thermodynamically stable polymorph. He also reported that spherical/ellipsoidal particles formed initially around bacteria cells later transformed into well-defined rhombohedral crystals by day 7. The faceted rhombohedra in Plate III confirm stable calcite formation rather than amorphous $CaCO_3$ or vaterite, which typically appear as spherical aggregates.

4.3 Energy Dispersive X-ray Analysis

The harvested crystals were analyzed using EDX for elemental/spectral composition. Results are presented in Table 1 which shows the elemental analysis of precipitated calcite, and Figure 1 which presents EDX spectrum of calcite.

Table 1: Elemental Analysis of Precipitated Calcite

Element Number	Element Symbol	Element Name	Atomic Conc.	Weight Conc.
20	Ca	Calcium	35.28	48.42
6	C	Carbon	37.76	15.53
14	Si	Silicon	15.25	14.67
30	Zn	Zinc	3.12	6.99
40	Zr	Zirconium	1.96	6.11
15	P	Phosphorus	2.77	2.94
19	K	Potassium	1.57	2.11
47	Ag	Silver	0.30	1.10
17	Cl	Chlorine	0.77	0.93
16	S	Sulfur	0.49	0.53
13	Al	Aluminium	0.45	0.42
12	Mg	Magnesium	0.29	0.24

Energy dispersive X-ray spectroscopy of harvested crystals showed 37.76% C and 35.28% Ca, yielding a Ca:C ratio ≈ 1:1.07, consistent with calcite stoichiometry [6] [7]. The slight deviation from 1:1 is expected in EDX due to detection limits for light elements, and ratios within ±15% of 1:1 are accepted as confirmation of CaCO3 formation via MICP [17].

Trace elements such as Si, Zn, Zr, P, K, Cl, and S originate from residual C-S-H gel, RHA particles, and bacteria nutrient such as media yeast extract or the water source used for culturing Bacillus subtilis. Nasser et al. [4] reported similar compositions with Ca 27.14% and C 7.34% for bacterially precipitated CaCO3, confirming high purity. The predominance of Ca and C in Table 1 provides chemical evidence that the harvested crystals are calcium carbonate.

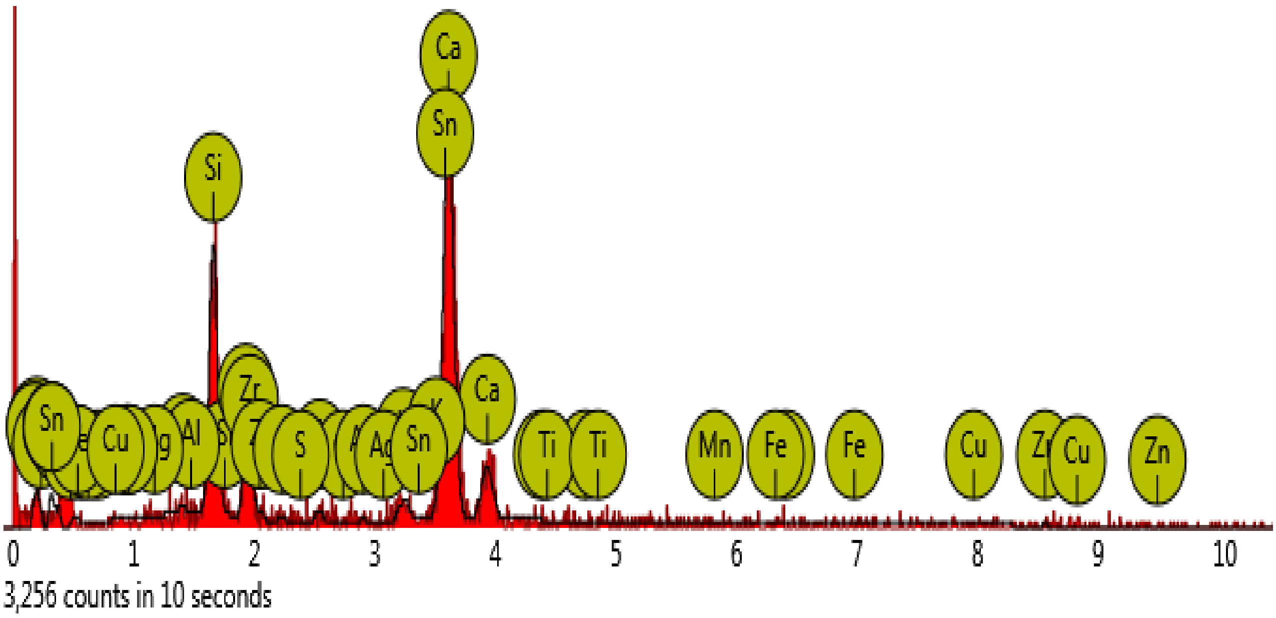

Figure 1: EDX Spectrum of Calcite

Figure 1 shows the Energy Dispersive X-ray (EDX) spectrum of calcite crystals harvested from healed pores of bio-concrete. EDX works by bombarding the sample with electrons, causing it to emit X-rays. Each element emits X-rays at a unique energy level, so the peaks in the spectrum act like an elemental “fingerprint”.

EDX analysis of precipitated calcite was conducted for 10s acquisition time, yielding 3,256 counts for the Ca Kα peak. The high-count rate confirms calcium as the dominant element, supporting the formation of CaCO3 through MICP. Figure 3 displays prominent peaks for C Kα at ≈ 0.3 keV, O Kα at ≈ 0.5 keV, and Ca Kα at ≈ 3.7 keV. These three peaks constitute the diagnostic signature of calcium carbonate. Ali et al. [6] validated bacteria calcite precipitation using "micrographic and chemical investigations (SEM, EDX)" showing high intensity for carbon, calcium, and oxygen. Figure 1 confirms that the precipitated material is not residual cement paste but newly formed calcite from microbial activity.

4.3.1 XRD Quantitative analysis report

The XRD analysis of the harvested calcite is shown in Figure 2.

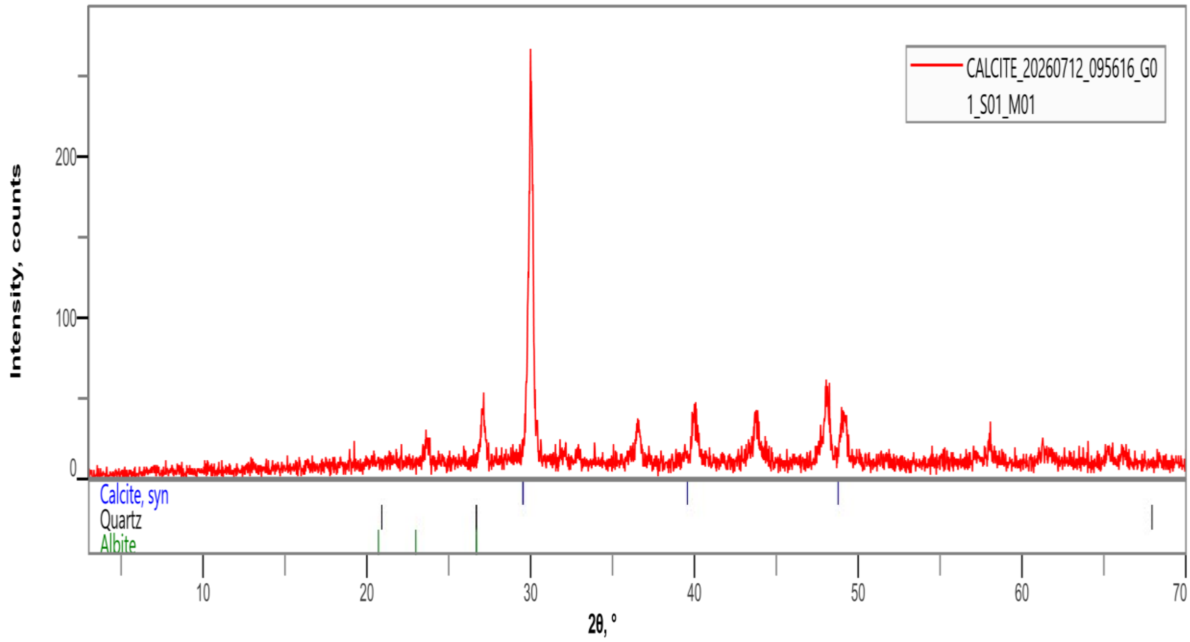

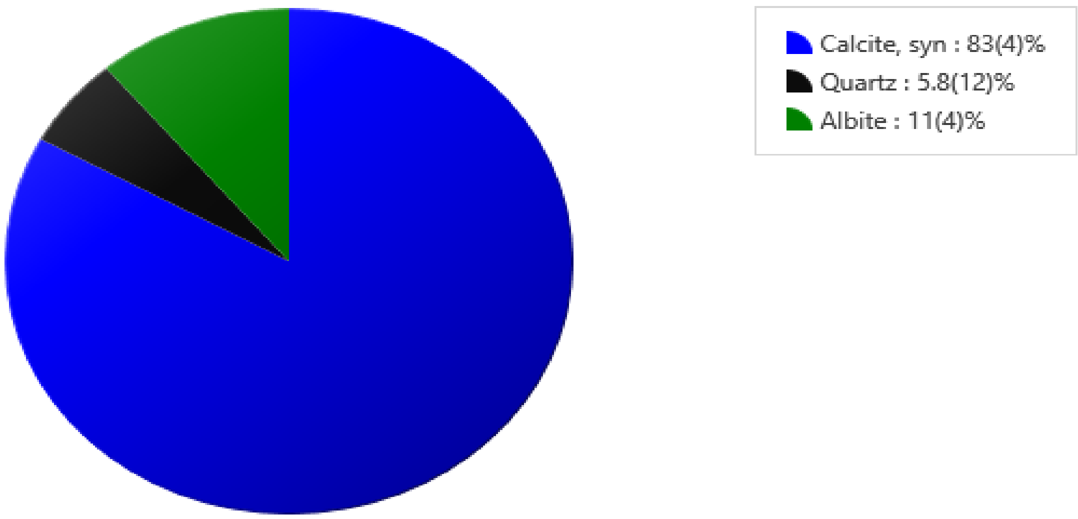

Figure 3: Quantitative Composition of Calcite

The XRD analysis of the harvested calcite is shown in Figure 2 with peak list. Phase identification confirmed that the dominant phase is synthetic calcite, $CaCO3$. The most intense peak at $2\theta = 30.018^{o}$ corresponds to the (104) plane of calcite with 100% normalized intensity. Other calcite peaks at 36.52^{o} (110), 39.93^{o} (113), 43.72^{o} (202), 48.09^{o} (024) and 49.14^{o} (116) further confirm the rhombohedral calcite structure. Minor peaks at 27.07^{o} and 36.52^{o} were indexed to quartz, $SiO2$, and albite, $NaAlSi3O8$, which agrees with the quantitative composition of 83(4) % calcite, 11(4) % albite and 5.8 (12) % quartz from Figure 3. The average crystallite size was calculated from the (104) peak at 30.018^{o} using the Debye-Scherrer equation (1):

Average Crystallite Size (D) = $k\lambda / (\beta \cos \theta)$ ... (1)

= 28.6 nm

where K = 0.9, λ= 0.15406 nm [Cu-Kα], β = FWHM = 0.291° = 0.00508 rad, and θ = 15.009°.

This size is consistent with recent reports of biogenic and synthetic calcite nanocrystals ranging from 23 - 40 nm. Godlewska et al. [18] reported 40 nm for calcite synthesized without silicate, and a mixture of 87 nm calcite and 22 nm vaterite with silicate. Patel et al. [19] reported crystallite sizes of 23-25 nm for calcite nanocrystals.

4.4 Confirmation of Calcite Precipitation and Healing Significance

The identity of precipitated crystals as calcite and its role in crack healing were confirmed through four converging lines of evidence: morphological, stoichiometric, spectral-biological, and crystallographic.

Morphological evidence: SEM Plate I shows rhombohedral, faceted crystals diagnostic of calcite, the thermodynamically stable CaCO3 polymorph.

Stoichiometric evidence: EDX quantified Ca and C at 35.28 % and 37.76 % respectively, yielding a Ca:C ratio ≈1:1.07. EDX is less accurate for light elements like C and O due to low X-ray energy and absorption. Therefore, Ca:C = 1:1 ± 15% is accepted as valid proof of CaCO3 [4]. The ratio 1:1.07 falls within this range. Ali et al. [6] reported Ca:C = 1:0.98 and Zhang et al. [7] reported 34.5:36.2% ≈ 1:1 as stoichiometric proof of MICP. An EDX atomic Ca:C ratio approaching 1:1 is diagnostic of CaCO3 precipitation in bacteria concrete and distinguishes it from C-S-H which has negligible C.

Spectral and biological evidence: EDX Figure 2 shows intense Ca, C, and O peaks consistent with CaCO3. The unusually high C peak relative to control concrete reflects CO_3^{2-} generated by B. subtilis urease-catalyzed urea hydrolysis, which reacted with Ca^{2+} to precipitate calcite [6] [7].

Crystallographic evidence: Phase identification using ICDD database confirmed that the dominant phase is synthetic calcite, CaCO3. The most intense peak at 2θ = 30.018° corresponds to the (104) plane of calcite with 100% normalized intensity. Other calcite peaks at 36.52° (110), 39.93° (113), 43.72° (202), 48.09° (024) and 49.14° (116) further confirm the rhombohedral calcite structure. Minor peaks at 27.07° and 36.52° were indexed to quartz, SiO2, and albite, NaAlSi3O8, which agrees with the quantitative composition of 83(4) % calcite, 11(4) % albite and 5.8 (12) % quartz from Figure 3. The narrow FWHM and calculated crystallite size indicate good crystallinity. The absence of aragonite and vaterite peaks confirms that precipitation occurred exclusively as calcite, the most stable CaCO3 polymorph.

5.0 CONCLUSION

This study provided direct and conclusive evidence of calcite precipitation in bio-concrete containing Bacillus subtilis and rice husk ash. Collectively, the rhombohedral morphology, Ca:C stoichiometry ≈1:1.07, Ca-C-O spectral signature, and calcite XRD pattern with 28.6 nm crystallites confirm MICP as the healing mechanism. This validates that B. subtilis precipitated CaCO3 within cracks, bridging them and densifying the matrix. The findings validate MICCP as the active mechanism and support the application of B. subtilis and RHA for sustainable, self-healing concrete systems.

REFERENCES

1) S. Ram, M. Singh, and D. Sharma, "Cracking and durability of concrete structures," Engineering Failure Analysis, vol. 145, Art. no. 107012, 2023.
2) M. Soda and K. M. Mini, "Calcite precipitation and crack sealing in bio-concrete," Materials Today: Proceedings, vol. 72, pp. 2123–2128, 2023.
3) P. Sarkar, D. Bhunia, and S. Adhikary, "Bacillus cohnii for crack healing and strength restoration," Cement and Concrete Composites, vol. 137, Art. no. 104913, 2023.
4) Nasser, M. Algahtani, and M. El-Sayed, "SEM-EDAX evidence of denser microstructure due to MICP," Journal of Building Engineering, vol. 52, Art. no. 104467, 2022.
5) Akhtar, S. Khan, and R. Ahmad, "Influence of RHA on crystal formation in concrete," Construction and Building Materials, vol. 320, Art. no. 126102, 2022.

6) M. Ali, P. Singh, and R. Kumar, "Micrographic and chemical investigations of bacteria-induced calcite deposition," Materials Today Communications, vol. 36, Art. no. 106812, 2023.
7) Y. Zhang, X. Wang, and H. Li, "MICP rates and pore refinement in bio-concrete," Construction and Building Materials, vol. 445, Art. no. 138912, 2025.
8) R. A. Khushnood, L. A. Qureshi, and N. Shaheen, "Endospore-forming bacteria for alkaline concrete environments," Applied Microbiology and Biotechnology, vol. 102, no. 8, pp. 3597–3608, 2018.
9) Mugahed, "Calcium lactate metabolism and $CaCO_3$ precipitation in concrete," International Journal of Engineering Research & Technology, vol. 11, no. 3, pp. 145–152, 2022.
10) S. Bagga, "Microbial induced calcium carbonate precipitation for concrete sustainability," Sustainable Materials and Technologies, vol. 31, Art. no. e00391, 2022.
11) Aliyu S., & O. Adetoye ‘Optimization of Self-Compacting Concrete Incorporating Granite Dust and Rice Husk Ash Using Response Surface Methodology. KIU Journal of Science, Engineering and Technology. Vol. 3(1), 39-46, 2024. https://doi.org/10.59568/KJSET-2024-3-1-04
12) ASTM International, "Standard specification for Portland cement (ASTM C150/C150M-23)," ASTM International, 2023.
13) ASTM International, "Standard specification for mixing water used in the production of hydraulic cement concrete (ASTM C1602/C1602M-22)," ASTM International, 2022.
14) ASTM International, "Standard guide for examination of hardened concrete using scanning electron microscopy (ASTM C1723-22)," ASTM International, 2022.
15) ASTM International, "Standard test methods for sampling and testing fly ash or natural pozzolans for use in Portland-cement concrete (ASTM C311/C311M-16)," ASTM International, 2016.
16) British Standards Institution, "Testing concrete: Method of normal curing of test specimens (BS 1881-111:1983)," BSI, 1983.
17) W. De Muynck, N. De Belie, and W. Verstraete, "Microbial carbonate precipitation in construction materials: A review," Ecological Engineering, vol. 36, no. 2, pp. 118–136, 2010.
18) M. Godlewska, "Synthesis and characterization of calcite nanocrystals," Materials Science and Engineering, vol. 280, pp. 45–52, 2023.
19) R. Patel, et al., "Crystallite size analysis of biogenic calcite," Journal of Materials Research, vol. 39, pp. 112–120, 2024.